# Growth and Dissolution of Succinic Acid Crystals in a Batch Stirred Crystallizer

Growth and dissolution of succinic acid crystals have been studied in an isothermal stirred tank crystallizer. Seeded desupersaturation and deundersaturation experiments have been performed. Parameters of a desired growth rate equation are estimated by fitting the supersaturation balance equation directly to the supersaturation measurements. The procedure is based on nonlinear optimization techniques. Thus, uncertainties in the traditional approximation of the concentration vs. time curve are circumvented. The growth process for succinic acid crystals in an aqueous solution is found to be controlled by a significant resistance in both the volume diffusion step and in the surface integration step. An implicit equation is given to accurately represent the crystal growth rate as a function of the supersaturation. When extrapolating outside the range of experiments, this equation is shown to predict growth rates that are significantly different from those predicted by a corresponding power law expression. The dissolution rate exhibits a nonlinear dependence on undersaturation which is interpreted as changes in the crystal shape. Initial dissolution rate coefficients are in good agreement with volume diffusion coefficients obtained from growth experiments.

**Yanfeng Qiu**
**Åke C. Rasmuson**
Department of Chemical Engineering
Royal Institute of Technology
S-100 44 Stockholm, Sweden

## Introduction

The crystal growth rate is an important parameter in the performance of industrial crystallizers. Unfortunately, growth rates measured in different laboratories differ significantly. Garside et al. (1975) plotted the linear face growth rates presented in the literature for potassium alum crystals. At the same supersaturation, the measurements differ by up to one order of magnitude. About the same spread in overall growth rates is found for potassium sulfate crystals (Palwe et al., 1984). The crystal growth rate depends on supersaturation, hydrodynamic conditions in the crystallizer, temperature, crystal size, impurities etc., allowing for different results from different measurements. To produce more reliable and useful data, experimental and evaluation techniques used for determination of crystal growth rates should be carefully examined and further improved. Very often a simple power law expression is used to correlate experimental results and to represent the growth rate in modeling. It is well known, however, that crystal growth is a two-step process: volume diffusion is followed by surface integration. The influence of temperature, hydrodynamics and impurities is different for the two steps. In the cases where both volume diffusion and surface integration are important, it is clearly desirable to separate them to improve the possibility to extrapolate to other conditions and to compare with other data. Methods to separate surface integration resistance from volume diffusion resistance are discussed by Garside et al. (1975). The most attractive one is to assume the volume diffusion rate at growth to be equal to the mass transfer rate at dissolution (Chianese et al., 1989; Scrutton and Grootscholten, 1981; Mullin and Whiting, 1980; Tavare and Chivate, 1979; Garside and Jancic, 1976; Phillips and Epstein, 1974; Garside et al., 1974; Garside and Mullin, 1968; Tanimoto et al., 1964; Ishii and Fujita, 1965). In some recent studies, the order of surface integration is just assumed to be equal to 2 and then the two-step model may be solved analytically for the growth rate and the rate constants are easily determined (Karpinski, 1981; Budz et al., 1984; Karpinski, 1985; Budz et al., 1985; Tai and Lin, 1987; Tai and Yu, 1989).

Correspondence concerning this paper should be addressed to A. C. Rasmuson.

There is a growing interest in using unstationary batch experiments for determination of crystal growth rates. The seeded desupersaturation experiment (Tanimoto et al., 1964; Bujac and Mullin, 1969; Jones and Mullin, 1973) provides a rapid way of obtaining the relation between crystal growth rate and supersaturation in the experiment. To an isothermal, supersaturated solution is added a certain amount of seed crystals, and the desupersaturation is recorded. By mass balance, the supersaturation decay is related to the crystal growth rate. Garside et al. (1982) derived a method to obtain the constants in the power law growth rate equation from only the initial derivatives of the desupersaturation curve. Palwe et al. (1985) estimate both nucleation and growth rate parameters from the desupersaturation curve. Measured values of the supersaturation vs. time are used directly in a nonlinear optimization. Halfon and Kaliaguine (1976) also discuss estimation of both nucleation and growth parameters from seeded isothermal desupersaturation experiments. Another approach in using batch experiments is to determine kinetics from measurements of the evolution of the crystal size distribution as suggested by Misra and White (1971) and as used in the S-plane analysis by Tavare and Garside (1986). In these methods the population balance is applied. Both the mass balance and the population balance are used in the analysis by Bransom and Dunning (1949) and by Verigin et al. (1979). This is also the case in a recent study by Klug and Pigford (1989). Measurements of the evolution of the crystal size distribution in isothermal batch experiments are used for determination of the growth rate and of the growth rate dispersion assuming surface integration to be the rate-controlling step.

Previous crystallization studies of succinic acid deal with crystal face growth rate measurements and overall growth and dissolution rate measurements on single crystals. Mullin and Whiting (1980) studied the growth of succinic acid crystals in aqueous solutions. The face growth rates were measured at different supersaturation, temperatures, solution velocities, and crystal orientations. Overall growth and dissolution rates of single crystals were measured under well-defined hydrodynamic conditions. Davey, Mullin, and Whiting (1982) performed growth experiments in water and isopropanol solutions to study the influence on the crystal habit. Crystals grown in aqueous solutions are plate-like with a dominant (001) basal plane. Growth in isopropanol solutions produced needle-like crystals. The face growth rates in both solutions were measured at different supersaturation.

The metastable range of succinic acid is comparatively narrow. The MSMPR technique, often used for determination of design data, is easily ruined by incrustations. In the present study, growth and dissolution rates of succinic acid crystals are determined at hydrodynamic conditions resembling the industrial situation and on a mass of crystals, making the results reasonably statistically founded. Seed crystals are added to an isothermal, supersaturated or undersaturated, stirred, aqueous solution, and the concentration is measured periodically during the experiment. Parameters of a desired growth rate equation are estimated by fitting the supersaturation balance equation directly to the supersaturation measurements using nonlinear optimization techniques. The evaluation is based on the two-step model for crystal growth, and the surface integration effectiveness factor is calculated. It is shown that the evaluation technique produces parameter values that are physically realistic and thereby allow themselves for further interpretation in terms of mechanisms. It is also shown that an improved evaluation as applied in this study is justified and even necessary to make laboratory experimental data more useful for industrial purposes. A simple power law gives an equally good correlation of experimental data, but predicts significantly different values when extrapolating outside the experimental range.

## Theoretical Studies

The growth of crystals in a solution is usually described as a two-step mechanism. Volume diffusion transports solute from the bulk solution to the crystal-solution interface, and surface integration denotes the integration of solute into the crystal lattice. These processes are usually described as acting in series. Each step is represented by a separate rate equation. For the diffusion of solute from the bulk to the interface, the rate equation is usually written:

$$G = k_d(c - c_i) \tag{1}$$

where $c$ and $c_i$ are concentrations in the bulk and at the interface, respectively. $k_d$ is the diffusion mass transfer coefficient and is a function of hydrodynamic conditions, transport properties of the solution and particle size. A number of studies have been performed to measure the mass transfer between a single sphere and a fluid. In the case of a stirred tank, Levins and Glastonbury (1972) recommend the equation:

$$\frac{k_c L}{D_v} = 2 + 0.47\left[\frac{L^{4/3}\epsilon^{1/3}}{\nu}\right]^{0.62}\left(\frac{D_s}{D_t}\right)^{0.17}\left(\frac{\nu}{D_v}\right)^{0.36} \tag{2}$$

for particles of near-neutral buoyancy. $k_c$ relates to mass transfer in terms of particle mass increase, while $k_d$ relates to an increase of the particle linear dimension as often used in crystallization. The relation between $k_c$ and $k_d$ can be written as:

$$k_c = \frac{3k_V}{k_A}\frac{\rho_c}{\rho}k_d \tag{3}$$

The surface integration of solute into the crystal lattice is a more complicated process. Based on the surface diffusion model, Burton et al. (1951) derived a well-known equation for crystal growth. Gilmer and Bennema (1972) have used a computer simulation technique to model crystal growth. It is assumed that single "ad-atoms" as well as clusters of ad-atoms and surface vacancies take part in the growth process. In a limited range of supersaturation, both of these models may be well represented by:

$$G = k_r(c_i - c^*)^r \tag{4}$$

where $r$ is between 1 and 2 for the surface diffusion model and between 0.83 and about 5 for the latter approach (Garside et al., 1975). The interfacial concentration $c_i$ in Eqs. 1 and 4 may be eliminated:

$$\frac{G}{k_d} + \left(\frac{G}{k_r}\right)^{1/r} = \Delta c \tag{5}$$

Equation 5 remains an implicit relation between the growth rate and the supersaturation except for $r = 1$ and 2. Often a simplifying power law equation:

$$G = k_g \Delta c^g \tag{6}$$

is used to relate the overall growth rate to the supersaturation. Usually, this equation is a good representation of Eq. 5 over a limited range of supersaturation. An important drawback, however, is that the simple power law equation does not allow for the fact that the influence of temperature and hydrodynamics are different for the two steps. As a consequence, significant errors may result when extrapolations are made to other conditions.

Crystal growth rates may be evaluated from seeded, isothermal desupersaturation experiments (Bujac and Mullin, 1969; Jones and Mullin, 1973). Consider a well-mixed, isothermal, batch crystallizer containing a solution initially supersaturated. To this solution is added seed crystals of uniform size. Assume that nucleation, breakage and agglomeration may be neglected. Then, supersaturation is consumed only by the crystal growth of seeds. The increase in the mass of crystals corresponds to the decrease in the solute concentration of the solution. Therefore, the mass balance for the solute can be written:

$$W - W_0 = M(\Delta c_0 - \Delta c(t)) \tag{7}$$

The mass of seed crystals is proportional to the cube of the crystal size. If the crystal shape remains unchanged and growth rate dispersion is negligible, the relation between the mass of crystals and their size can be expressed as:

$$\frac{W}{W_0} = \left(\frac{L}{L_0}\right)^3 \tag{8}$$

From Eqs. 7 and 8, the supersaturation during the experiment is:

$$\Delta c(t) = \Delta c_0 - \left[\left(\frac{L}{L_0}\right)^3 - 1\right]\frac{W_0}{M} \tag{9}$$

Since the linear crystal growth rate is defined as:

$$G(\Delta c) = \frac{dL}{dt} \tag{10}$$

a differentiation of Eq. 9 in time creates a relation between measured concentrations and the growth rate. The time derivative of the supersaturation is obtained from a function correlating measured supersaturation vs. time. The function used is usually a polynomial (Bujac and Mullin, 1969; Jones and Mullin, 1973). We have found that the method of correlation may have a significant influence on the calculated growth rates. Furthermore, simple polynomials usually do not behave well close to the boundaries and outside the range of experimental data. This is usually seen in the low supersaturation end (Palwe et al., 1985) and reduces the range over which reliable growth rates may be calculated. We propose here a method which circumvents these problems. Instead of differentiating Eq. 9, we integrate Eq. 10. Assuming a certain growth rate equation, such as Eq. 5 or 6, the crystal size at time $t$ can be calculated as:

$$L = L_0 + \int_0^t G(\Delta c)\, dt \tag{11}$$

Using Eq. 11, the kinetic parameters in the growth rate equation is estimated by fitting Eq. 9 directly to the experimental supersaturation measurements. This allows us to use only the actually measured supersaturation values. Instead of differentiating the experimental desupersaturation curve, we integrate a mathematical function given to represent the growth rate vs. supersaturation. The problem becomes a nonlinear parameter estimation of a dynamic model (Bard, 1974). The optimization is defined as minimizing the sum of squares of the supersaturation residuals:

$$F = \sum_{j=1}^{m} (\Delta c(t_j) - \Delta c_j)^2 \tag{12}$$

The NAG library subroutine E04FCF which applies a combined Gauss-Newton and quasi-Newton method has been used successfully in this study for the optimization. A subroutine to calculate $\Delta c(t_j)$ is supposed to be furnished by the user. In this routine, the chosen growth rate function is used in Eq. 11 to calculate the size which is inserted in Eq. 9. The NAG subroutine itself calculates the derivatives used in the optimization process. Also the routine E04GDF may be used and then the partial derivatives of $\Delta c(t)$ with respect to the kinetic parameters, $k_i$, have to be given:

$$\frac{\partial \Delta c(t)}{\partial k_i} = \frac{d\Delta c(t)}{dL}\frac{\partial L}{\partial k_i} \tag{13}$$

Using Eq. 9 and 11:

$$\frac{\partial \Delta c(t)}{\partial k_i} = -\frac{3}{L_0}\left(\frac{L}{L_0}\right)^2 \frac{W_0}{M}\int_0^t \frac{\partial G(\Delta c)}{\partial k_i}\, dt \tag{14}$$

Numerical integration is needed to evaluate both the residual function and derivatives.

## Experimental Studies

The experiments are performed in a 2.5-L, jacketed, glass crystallizer. The crystallizer is shown in detail in Figure 1. Three vertical baffles are installed, and the impeller is of the propeller type with three blades. All dimensions are given in millimeters. A constant temperature bath supplies water to the jacket of the crystallizer to keep the temperature within ±0.02°C of the desired value.

The supersaturated solution is prepared from recrystallized crystals of commercial succinic acid. Crystals are dissolved in distilled water. The solution is charged into the crystallizer and a sample for determination of the initial concentration is taken out. The initial supersaturation is achieved by slow cooling. When the experiment temperature is attained, the stirrer speed is adjusted to the maximum level, 710 rpm, to allow for immediate dispersion of the seeds into the solution. A known amount of closely-sized seed crystals is charged to the crystal-

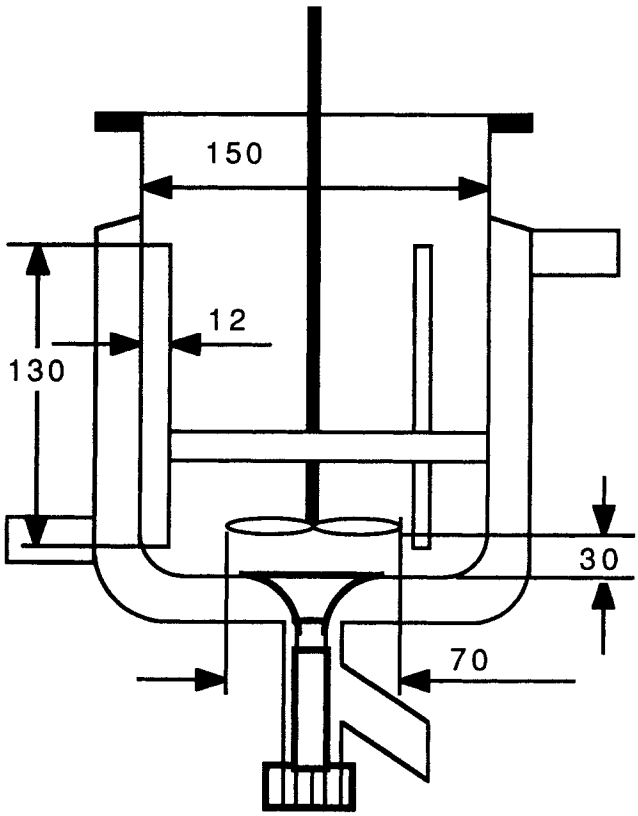


**Figure 1. Crystallizer**

lizer. The rotation speed of the stirrer is immediately adjusted to the desired level. Using 10-mL glass pipettes, small samples of clear solution are withdrawn periodically (every 10 minutes) for concentration analysis. The first sample is taken 5 min after the addition of the seeds. On the tip of the pipette, a cotton plug is fitted to prevent crystals from being sucked into the pipette. At the end of the experiment, the suspension is filtered and the product is dried for microscopic inspection.

The seed crystals are prepared by dissolving commercial succinic acid crystals in water and then performing a cooling crystallization. The product is carefully sieved, and the fractions 355–400, 560–630 and 710–800 (DIN 4188) have been used. The seed size, $L_0$, of each range is taken as the geometric mean. The shape of succinic acid crystals grown from aqueous solutions is described by Mullin and Whiting (1980) as resembling a six-sided prism with a large predominant basal plane. The shape of the seed crystals fits well to this description and to the figure shown in the previous study. The crystals are flat, but still rather chunky.

The concentration of the solution is determined by measuring the density using an Anton Paar DMA 60 density meter. The temperature in the measuring cell of the density meter is kept constant by circulating constant temperature water from a bath. The temperature stability of the bath is ±0.002°C. The relation between density and concentration for a succinic acid–water solution is determined:

*At 29.90°C:*

$$c = -1.371 \times 10^{-3} + 3.52269 \times 10^{-3}(\rho - \rho_w) + 7.112 \times 10^{-6}(\rho - \rho_w)^2 \quad (15)$$

*At 36.97°C:*

$$c = 7.98 \times 10^{-5} + 3.4191 \times 10^{-3}(\rho - \rho_w) + 1.2665 \times 10^{-5}(\rho - \rho_w)^2 \quad (16)$$

The sample from an experiment is supersaturated. In order to avoid crystallization in the density meter the temperature at analysis should be kept high enough to assure that the sample becomes undersaturated in the instrument. Accordingly, the instrument is temperature-controlled to a temperature above the experiment temperature and the density–concentration calibration is done at this temperature. Equation 15 is used for experiments performed at 22.0°C and Eq. 16 for experiments at 28.0°C.

The solubility of succinic acid in water has been measured in the temperature range 20°C to 41.9°C. The apparatus consists of a sealed glass flask fitted with a stirrer and is immersed in a constant temperature bath, controlled to ±0.01°C. Equilibrium was achieved from both supersaturated and undersaturated solutions. At some temperatures, two measurements were made and the mean values were calculated. At other temperatures, more than six measurements were made, and the mean and the 95% confidence interval were calculated. The temperatures were measured in the water bath to at least ±0.05°C. The results are presented in Table 1 and are in good agreement with data reported earlier by Mullin (1972), Seidell (1958), and Stephen and Stephen (1963).

The range over which experimental parameters can be varied conveniently is limited. The density of succinic acid crystals is just slightly higher than that of water. Accordingly, the efficiency of dispersing the seeds into the solution decreases with decreasing size. The desupersaturation rate has to be reasonable as well as the size change. Secondary nucleation becomes significant if the experiment time is too long or the supersaturation is too high. The size increase in growth experiments range from 29 to 166 μm as calculated from the mass change. The size decrease in dissolution experiments range from 110 to 180 μm.

A total of 31 growth experiments and six dissolution experiments have been conducted. The growth experiments comprise two temperatures, three stirring rates, and three seed sizes, Table 2. The range of dissolution experiments is given in Table 3. The amount of solvent, i.e., water, is in all experiments 2.5 kg.

**Table 1. Solubilities of Succinic Acid in Water**

| Temp. °C | Solubility ±95% Confidence Limits kg/kg Water |
|---|---|
| 20.0 | 67.16 |
| 22.0 | 73.69 |
| 24.0 | 80.32 |
| 25.9 | 87.36 ± 0.12 |
| 27.9 | 95.68 ± 0.32 |
| 29.9 | 103.43 |
| 31.9 | 113.07 ± 0.21 |
| 33.9 | 123.16 ± 0.28 |
| 35.95 | 134.00 ± 0.25 |
| 38.00 | 146.40 ± 0.53 |
| 39.9 | 158.28 ± 0.13 |
| 41.90 | 171.88 ± 0.19 |

Table 2. Parameters Used in Growth Experiments

| Parameters | Ranges | Units |
|---|---|---|
| Supersaturation $\Delta c$ | 0.3–5.25 | g/kg water |
| Seed Size | 355–400, 560–630, 710–800 | $\mu$m |
| Impeller Speed | 400, 550, 710 | rpm |
| Temperature | 22.0 ± 0.03, 28.0 ± 0.03 | °C |
| Amount of Seeds | 5–10 | g |
| Experimental Time | 5,100 | s |

## Results and Evaluation

The optimization calculations are performed in double precision FORTRAN. For the numerical integration of Eq. 11, Heun's method (Dahlquist and Björck, 1974) is used with a time step of 5 seconds. Smaller time steps do not improve significantly. Since the desupersaturation balance is an ordinary differential equation, an initial condition has to be given in the optimization. The initial supersaturation of each experiment is used as the initial condition for the integration. The approximate 95% confidence limits are evaluated (Draper and Smith, 1981) to examine the reliability of the estimated values.

In Table 4 is given some of the results on the three parameters ($k_d$, $k_r$ and $r$) of the growth rate for each experiment as estimated in Eq. 5. Obviously the values change considerably, and the reproducibility is low. In some cases the confidence limits of the parameters are very large, but in all cases, the experimental desupersaturation data points are fitted very well. In Figure 2 is shown supersaturation measurements of an experiment and the desupersaturation curve that corresponds to the result of the optimization process. Obviously, no peculiar end effects appear as is the case when a polynomial is used for correlation of the desupersaturation measurements. To examine the experimental reproducibility, the growth rate vs. supersaturation (Eq. 5) curves of six experiments at the same seed size, temperature and impeller speed are compared in Figure 3. The seed amount ranges from 6 to 8 g. There is no clear influence of the amount of seeds. The experimental reproducibility leaves an uncertainty of 10–20% in the growth rate values, except at very low supersaturation where the relative uncertainty may become much larger. This experimental uncertainty may be related to the precision in supersaturation measurements, being approximately ±0.3 g/kg. Furthermore, the properties of the seed crystals are not perfectly reproducible.

The number of supersaturation measurements in each experiment is 10, which is rather low in comparison to that of regression parameters. This may partly explain why confidence intervals of the parameters are rather wide. Furthermore, Eq. 5 does not show a strong curvature in growth rate vs. supersaturation in a log-log diagram. Therefore, the problem of distinguishing between the effect of mixed resistances and that of $r$ deviating from unity is very difficult. In optimization terminology, it means that the $F$ (Eq. 12) contours are greatly elongated. In fact, by using the method of polynomial correlation of the desupersaturation data and then calculating growth rates for evaluation of growth rate function parameters, it seems to be impossible to separate these two effects. We were not able to find an adequate minima in the optimization when using data from several experiments, all at the same stirring rate. The minimization process was very slow and unrealistic volume diffusion mass transfer rate coefficients resulted. The experimental desupersaturation curves can be fitted very well by Eq. 9, also when the growth rate is represented by the power law, Eq. 6. The parameter values so obtained, however, show the same lack of reproducibility. Although the kinetic parameters in Table 4 change considerably, it is clearly shown that $k_d$ increases with impeller rotation speed as is expected.

To use measured supersaturation values directly, without initially correlating them to a function, was suggested by Palwe et al. (1985). In their treatment they allowed for consumption of supersaturation both by growth and by nucleation, and crystal

Table 3. Parameters Used in Dissolution Experiments

| Parameters | Ranges | Units |
|---|---|---|
| Undersaturation | 0.5–4.0 | g/kg water |
| Seed Size | 710–800 | $\mu$m |
| Impeller Speed | 400, 550, 710 | rpm |
| Temperature | 22.0 ± 0.03 | °C |
| Amount of Seeds | 13–18 | g |
| Experimental Time | 1,500–3,300 | s |

Table 4. Examples of Kinetic Parameters from Nonlinear Least Squares, Eq. 5*

| $N$ | $W_0 \times 10^3$ | $k_d$ | $k_r$ | $r$ |
|---|---|---|---|---|
| 400 | 6 | 3.97 ± 1.33 | 120 ± 1630 | 4.63 ± 13.00 |
| | 6 | 5.64 ± 1.33 | 2.63 ± 1.55 | 4.13 ± 2.27 |
| | 7 | 3.89 ± 1.00 | 14.0 ± 43.6 | 3.99 ± 4.34 |
| | 7 | 4.31 ± 1.09 | 15.4 ± 48.3 | 4.06 ± 4.33 |
| | 8 | 5.76 ± 4.33 | 4.55 ± 5.92 | 1.99 ± 1.16 |
| | 8 | 4.40 ± 1.35 | 10.3 ± 27.9 | 3.83 ± 3.93 |
| 550 | 6 | 6.90 ± 7.87 | 2.15 ± 4.05 | 4.05 ± 8.27 |
| | 6 | 9.14 ± 6.93 | 2.20 ± 1.16 | 2.59 ± 1.35 |
| | 8 | 7.70 ± 1.63 | 1.20 ± 0.16 | 3.56 ± 0.81 |
| | 8 | 6.85 ± 2.13 | 2.57 ± 1.62 | 3.78 ± 1.85 |
| 710 | 6 | 8.83 ± 2.44 | 3.36 ± 1.43 | 3.06 ± 0.82 |
| | 6 | 8.23 ± 3.53 | 6.53 ± 13.1 | 4.30 ± 4.20 |
| | 8 | 10.1 ± 5.1 | 2.34 ± 1.12 | 2.94 ± 1.17 |
| | 8 | 6.78 ± 1.91 | 4.85 ± 8.57 | 5.89 ± 5.19 |

*±95% confidence limits; $G$, $10^8$ m/s (for this table only); $\Delta c$, g/kg water (for this table only); $T = 22.0$°C; $L_0 = 595$ $\mu$m

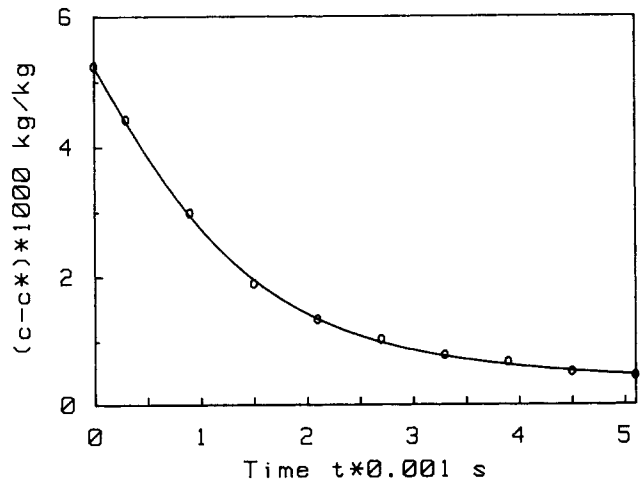


**Figure 2. Measured desupersaturation curve (point) and calculated curve (solid line) using estimated constants of Eq. 5 obtained by optimization.**

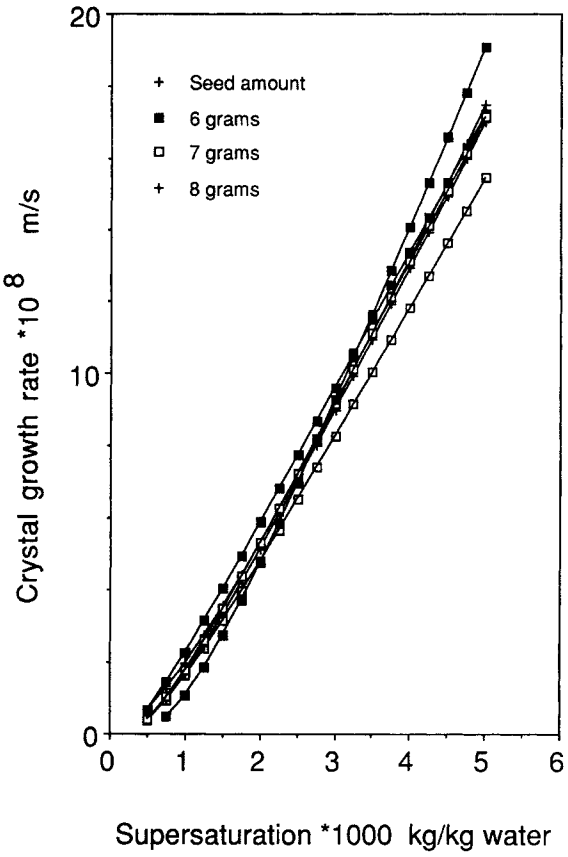


**Figure 3. Experimental reproducibility.**

growth was evaluated in terms of a power law expression. Unfortunately, this nonlinear optimization was not very successful in correlating measured supersaturation values. It is not clear if this is due to difficulties in the optimization or inadequate representation of kinetics. Furthermore, assigning a mass to crystal nuclei involves particular problems. In comparison to Table 4, Palwe et al. (1985) also found a significant scatter in comparing results from different individual runs. No attempt was made to use results from more than one experiment in the same regression.

The mean power input, $\epsilon$, is usually assumed to be proportional to the third power of the stirring rate (Oldshue, 1983). The Sherwood number of 500 $\mu$m particles at 400 rpm is approximately 30. Neglecting the first term in Eq. 2 results in:

$$k_c \propto N^{0.62} L^{-0.17} \tag{17}$$

Obviously the influence of size on the volume diffusion mass transfer rate is not very strong. Furthermore, the size range actually covered in the experiments is not very extensive. Including just the influence of the stirring rate in Eq. 5 results in:

$$\frac{G}{k_{d0}(N/400)^{0.62}} + \left(\frac{G}{k_r}\right)^{1/r} = \Delta c \tag{18}$$

Equation 18 is used for parameter estimation based on all experiments at each temperature. The results are given in Table 5. The parameters are now much more reliable as seen from the confidence intervals. Figures 4 and 5 show the deviations

**Table 5. Values of Parameters for Eq. 18***

| $n$ | $T$ | $k_{d0} \times 10^5$ | $k_r$ | $r$ | $F \times 10^6$ |
|---|---|---|---|---|---|
| 26 | 22.0 | 5.407 ± 0.745 | (3.437 ± 1.556)·10$^4$ | 3.990 ± 1.120 | 5.663 |
| 5 | 28.0 | 10.02 ± 8.95 | 0.599 ± 0.327 | 2.482 ± 1.114 | 3.269 |

* ± 95% confidence limits

between measured supersaturation and those predicted by Eq. 18. The goodness of fit is lower than shown in Figure 2 since one equation is used to represent 26 and five experiments, respectively. The experimental initial supersaturation of each experiment has been used as initial condition. A regression on 26 experiments needs 26 initial conditions. The residuals in Figures 4 and 5 are usually less than 0.4 g/kg water.

As shown in Eq. 17, $k_d$ is approximately proportional to $L^{-0.17}$. The size influence on the surface integration step is more difficult to predict in advance. Rather strong influence has been shown in certain cases (Jancic and Grootscholten, 1984), particularly at smaller sizes. Normally, $k_r$ increases with size. The influence of temperature may be accounted for by Ahrrenius-type equations for the rate constants. The diffusivity is approximately directly proportional to temperature and inversely proportional to the dynamic viscosity. Using bulk-phase data for pure water and Eq. 2, the activation energy for volume diffusion is estimated to $E_v$ = 16.7 kJ/mol. It is within the range of experimental values: 5 to 20 kJ/mol (Tavare and Chivate,

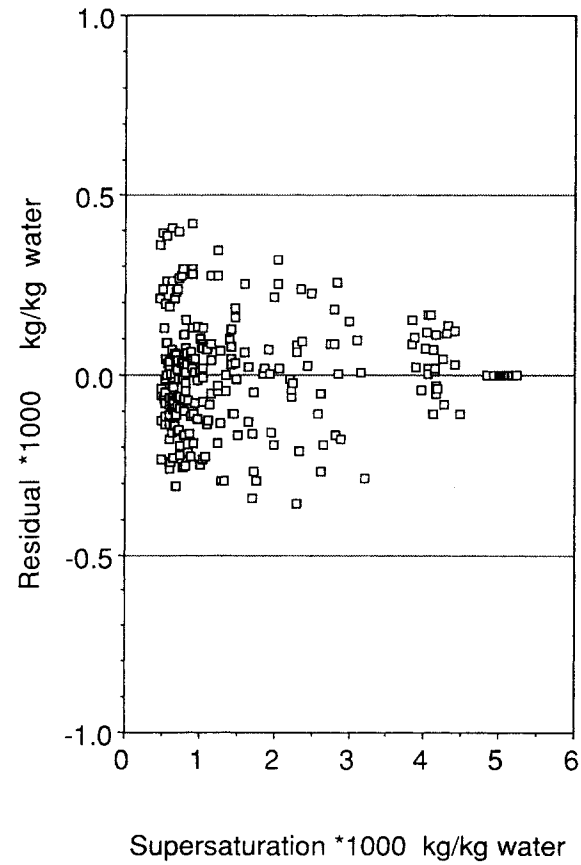


**Figure 4. Goodness of fit of Eq. 18 to all experiments of 22.0°C.**

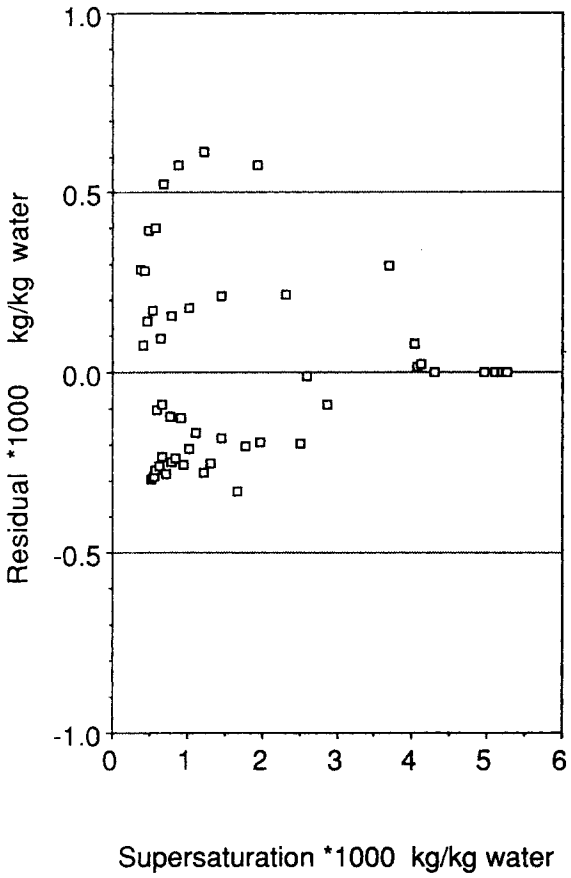


**Figure 5. Goodness of fit of Eq. 18 to all experiments of 28.0°C.**

1979; Scrutton and Grootscholten, 1981; Garside and Mullin, 1968; Garside et al., 1974) and of theoretical values: 12 to 30 kJ/mol (Mullin and Gaska, 1969). Taking temperature and size effects into consideration, the crystal growth rate equation can be expressed as:

$$\frac{G}{k_{d0}(N/400)^{0.62}L^{-0.17}\exp(-E_v/RT)} + \left(\frac{G}{k_{r0}L^b\exp(-E_r/RT)}\right)^{1/r} \Delta c \quad (19)$$

In Table 6 is shown the results of five-parameter optimization of Eq. 19 to determine: $k_{d0}$, $k_{r0}$, $b$, $E_r$, and $r$ for different values of $E_v$. All experimental results have been used comprising 31 experiments and over 300 measured supersaturation values. As compared to Eq. 18, an improvement in confidence limits is obtained and the increase in the sum of squared residuals is small even though the number of data points is increased. Above the volume diffusion activation energy was estimated to be 16.7 kJ/mol. The goodness of fit of Eq. 19 for this value is revealed in Figure 6. Based on Eq. 19, the order of surface integration with respect to supersaturation is found to be approximately 3. The surface integration process is significantly size-dependent to order 1.6 and the activation energy is approximately 16 kJ/mol. From Table 6 it may be concluded that the goodness of fit is rather uninfluenced by the value adopted for the volume diffusion activation energy. Actually, a nearly equally good fit is obtained if the size and temperature influence on volume diffusion is neglected completely. Furthermore, this would not influence significantly: the volume diffusion to surface integration resistance ratio; the values of the rate constants, $k_d$ and $k_r$; and the order of the surface integration with respect to supersaturation, $r$, and with respect to size, $b$. Only the influence on the surface integration activation energy is significant.

To examine the relative influence of volume diffusion and surface integration, the surface integration effectiveness factor (Garside, 1971):

$$\eta_r = \frac{\text{Measured Overall Growth Rate}}{\text{Growth Rate When Crystal Surface Is Exposed to Conditions in Bulk Solution}} = \frac{G}{k_r(c-c^*)^r} \quad (20)$$

is calculated using Eq. 19. The denominator in Eq. 20 includes factors accounting for size and temperature dependence of the surface integration step. The results are shown in Figure 7. Theoretically, the effectiveness factor ranges from zero to unity. Unity means that the process is fully surface-integration-controlled. Figure 7 shows that the process becomes more surface-integration-controlled as the seed crystal size decreases and as the stirring rate increases. The influence, however, is not very strong. The influence of supersaturation on the effectiveness factor is much stronger. At low supersaturation, around 1 g/kg water, the effectiveness factor is about 0.6 implying that both steps are about equally important. At high supersaturation, the effectiveness factor declines to about 0.1 The volume diffusion resistance dominates. The activation energy for surface integration is close to the corresponding value for volume diffusion. Accordingly, the relative influence of the two steps remains essentially constant as the temperature changes. In Figure 7, the effectiveness factor curves at 22°C and 28°C of 595 $\mu$m crystals at 400 rpm coincide.

In evaluating the dissolution kinetics it is assumed that the

**Table 6. Values of the Parameters for Eq. 19***

| $E_v \times 10^{-3}$ | $k_{d0} \times 10^4$ | $k_{r0} \times 10^{-9}$ | $r$ | $b$ | $E_r \times 10^{-3}$ | $F \times 10^6$ |
|---|---|---|---|---|---|---|
| 5 | 1.588 ± 0.228 | 3,223 ± 983 | 2.994 ± 0.393 | 1.547 ± 0.403 | 35.63 ± 16.06 | 5.949 |
| 10 | 11.97 ± 1.685 | 170.1 ± 51.7 | 3.025 ± 0.400 | 1.584 ± 0.413 | 27.17 ± 15.01 | 5.872 |
| 15 | 90.63 ± 12.53 | 7.386 ± 2.215 | 3.046 ± 0.404 | 1.611 ± 0.418 | 18.59 ± 14.41 | 5.806 |
| 16.7 | 177.1 ± 24.4 | 2.540 ± 0.757 | 3.050 ± 0.404 | 1.618 ± 0.419 | 15.77 ± 14.32 | 5.787 |
| 20 | 688.7 ± 93.8 | 0.2871 ± 0.0843 | 3.056 ± 0.404 | 1.629 ± 0.420 | 10.10 ± 14.30 | 5.752 |

* ±95% confidence limits

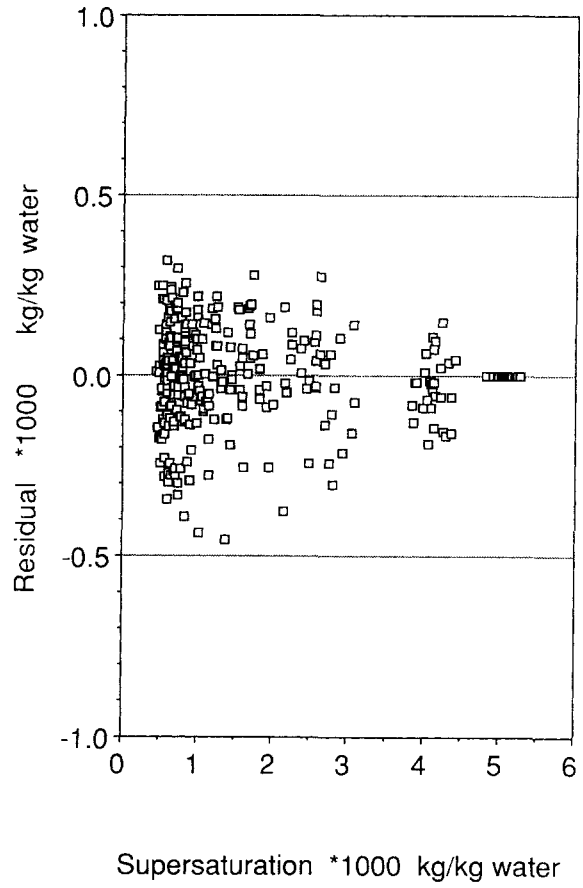


**Figure 6. Goodness of fit of Eq. 19 to all experiments, $E_v = 16.7$ kJ/mol.**

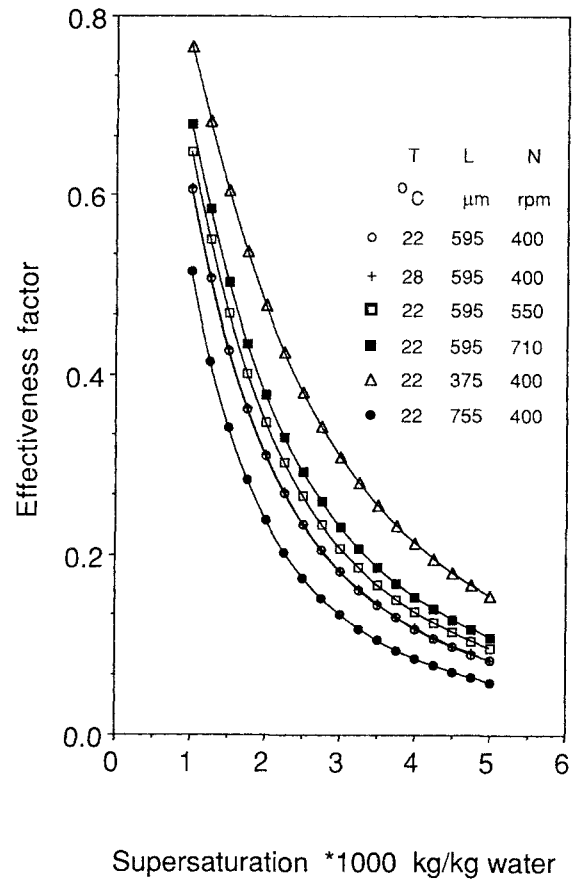


**Figure 7. Surface integration effectiveness factor, $E_v = 16.7$ kJ/mol.**

only resistance to dissolution is limitations in volume diffusion rate. The influence of crystal size is neglected. The dissolution rate is expressed as:

$$D = k_D \Delta c \tag{21}$$

However, Eq. 21 is not able to represent the data satisfactorily. Actually, the data correspond to a nonlinear relation between dissolution rate and driving force. A power law:

$$D = k'_D \Delta c^d \tag{22}$$

fits the experimental data well. Equation 22 has been correlated to the undersaturation measurements of each experiment separately and the results are shown in Figure 8. The dissolution rate decreases stronger than just proportionally to the driving force as the undersaturation decreases during the experiment. In terms of Eq. 21, the dissolution rate constant decreases by up to a factor of about 3. Since the change in concentration is rather small during an experiment, the nonlinearity is not likely to be explained by a concentration-dependent diffusivity. Nor is the size change very large, and even so volume diffusion would be expected to increase with decreasing size. The size change at dissolution is in the order of 150 $\mu$m (seed size 710–800 $\mu$m). The change in $k_D$ is probably due to changes in shape of crystals during dissolution. By microscopy we have observed that the crystals during dissolution become rounded and lose their characteristic shape. Also, the surface of the crystals, most clearly observable on the dominating plane 001, become rather rough during dissolution. In the beginning of an experiment, the seeding material contains nearly perfect crystals and some crystals that are broken. During dissolution, the corner and edges are dissolve faster and disappear early. The surface area shape factor decreases during the experiment and probably also the shape change influences the hydrodynamics around the particle. The overall dissolution mass transfer rate decreases as the crystals become more and more rounded. Then only the dissolution rate constant in the beginning of each experiment is of interest for comparison with the volume diffusion rate constant during growth. Table 7 presents the initial dissolution mass transfer rate coefficient of each experiment and the corresponding volume diffusion mass transfer coefficient of Eq. 19. The agreement between dissolution and growth values is good. The dissolution mass transfer coefficients vs. stirring rate fits rather well to the exponent of 0.62 used in evaluating the growth data.

## Discussion

The fact that the mass transfer rates obtained from the dissolution of fresh, well-shaped crystals are reasonably close to the volume diffusion mass transfer rate constants at growth supports a conclusion that the parameters determined from the growth experiments have a physical relevance. It is encouraging since the growth parameters result from a direct five-parameter

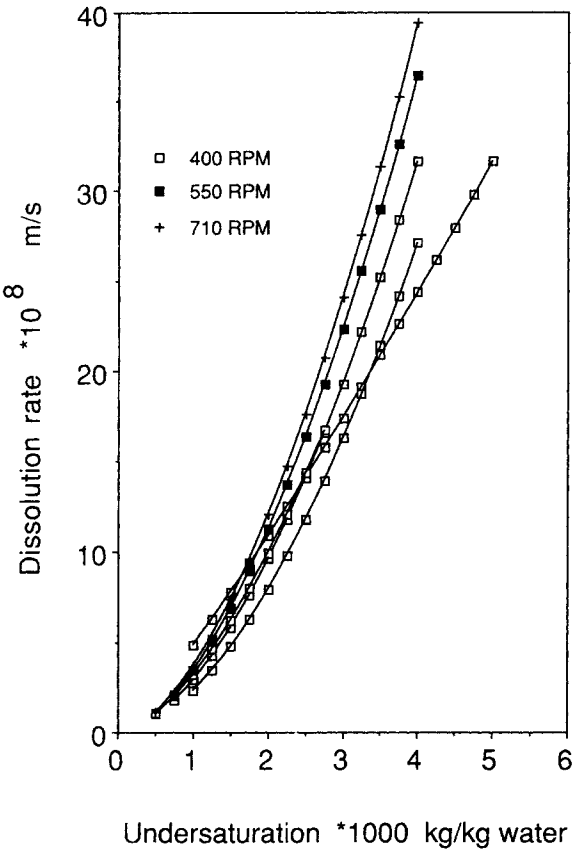


**Figure 8. Dissolution rates assuming a constant shape factor.**

nonlinear optimization based on awkward supersaturation measurements and somewhat scattered experimental results. Below we discuss each parameter separately and possible conclusions concerning the particular growth process.

Mullin and Whiting (1980) determined for succinic acid in aqueous solution, overall growth rate and face growth rates of fixed single crystals at 21, 27 and 35°C. From the temperature dependence of the growth rate of an individual face, the activation energy is determined to 18 kJ/mol. This value relates to an overall power law expression, and accordingly it contains the influence of temperature both on volume diffusion and on surface integration. The surface integration activation energy determined by us is approximately 16 kJ/mol. This value, however, depends significantly on the value adopted for the volume diffusion activation energy as shown in Table 6, and the range of 95% confidence limits is wide. Completely neglecting the temperature dependence of the volume diffusion step results in an activation energy for surface integration of 48 kJ/mol. In using a simple crystal overall power law expression to correlate our results, Eq. 23, we obtain the same value as Mullin and Whiting (1980) did for the overall face activation energy. Sixteen kJ/mol is within the range of surface activation energies found for other substances; for instance, 14.8 for sodium chloride (Scrutton and Grootscholten, 1981), 40.88 for potassium sulfate (Tavare and Chivate, 1979), 43 and 52 for potash alum (Garside and Mullin, 1968; Garside et al., 1974). The value on $E_r$ determined by us is reasonable, but approximate.

**Table 7. Dissolution Coefficient vs. Volume Diffusion Coefficient**

| $N$ | $\Delta c_0 \times 10^3$ | From Eq. 22 $k_D \times 10^5$ | From Eq. 19* $k_d \times 10^5$ |
|---|---|---|---|
| 400 | 5.06 | 6.340 | 6.633 |
| 400 | 3.83 | 7.682 | |
| 400 | 2.70 | 6.138 | |
| 400 | 3.96 | 6.731 | |
| 550 | 4.07 | 9.213 | 8.081 |
| 710 | 4.11 | 10.04 | 9.467 |

*$E_r$ = 16.7 kJ/mol, $T$ = 22°C, $L = 0.755 \times 10^{-3}$ m

Mullin and Whiting (1980) found the overall crystal growth rate to be of order 1.38 with respect to supersaturation. Using a measured dissolution rate constant, the order of surface integration is determined to 1.8 for supersaturation up to about 3 g/kg. At higher supersaturation, a scatter in the data points indicates an order exceeding 2. In comparison, we obtain a surface integration order of approximately 3 using data from about 1 g/kg to 5 g/kg in supersaturation. Mullin and Whiting (1980) conclude that the surface diffusion mechanism dominates. In the surface diffusion model of Burton et al. (1951) the order of the integration process range from unity to 2. In the nuclei above the nuclei model of Gilmer and Bennema (1972), the range is from 0.83 to 5. In both models, the order decreases as the supersaturation increases. Therefore, an increase in the order of growth at increasing supersaturation is likely to be related to a transition in mechanism. Our higher value on the order of surface integration suggests that the surface nucleation mechanism dominates in our experiments. This is reasonable since our range of data include higher supersaturation, and Mullin and Whiting (1980) observed a transition in mechanism in the upper end of their data. Order of surface integration exceeding 2 has been reported for other substances, for instance, 2.61 (Tavare and Chivate, 1979) and 2.4 (Garside et al., 1974) for potassium sulfate.

The rate constants for dissolution and for the volume diffusion step at growth range from about $6.3 \times 10^{-5}$ m/s at 400 rpm to about $10.0 \times 10^{-5}$ m/s at 710 rpm in the present study. Mullin and Whiting (1980) report an overall dissolution rate constant of 0.0328 [kg/m$^2$ s (kg/kg)] for a crystal-solution relative velocity of 0.2 m/s. From the shape information in the paper, the volume and area shape factors are estimated to $k_V = 0.330$ and $k_A = 2.18$, when the second largest dimension is used to characterize the size. Using these values their dissolution rate constant is recalculated to $4.59 \times 10^{-5}$ m/s. Differences in hydrodynamic conditions, crystal size, and possibly in shape contribute to differences in dissolution rates. Furthermore, we only use the initial value of the dissolution rate constant of each experiment since a significant decrease occurred during the process. The overall growth rate equation given by Mullin and Whiting (1980) applies to 27.3°C and may be compared with Eq. 19 at this temperature. The denominator in the volume diffusion term, Eq. 19, is replaced by their recalculated dissolution mass transfer rate constant to account for differences in hydrodynamics. In Figure 9, Eq. 19 is plotted for different assumed sizes with the results of Mullin and Whiting. Since they used much bigger crystals than in the present study, the results are in reasonable agreement.

It has been shown that growth rate dispersion and size-dependent growth create similar effects and are difficult to

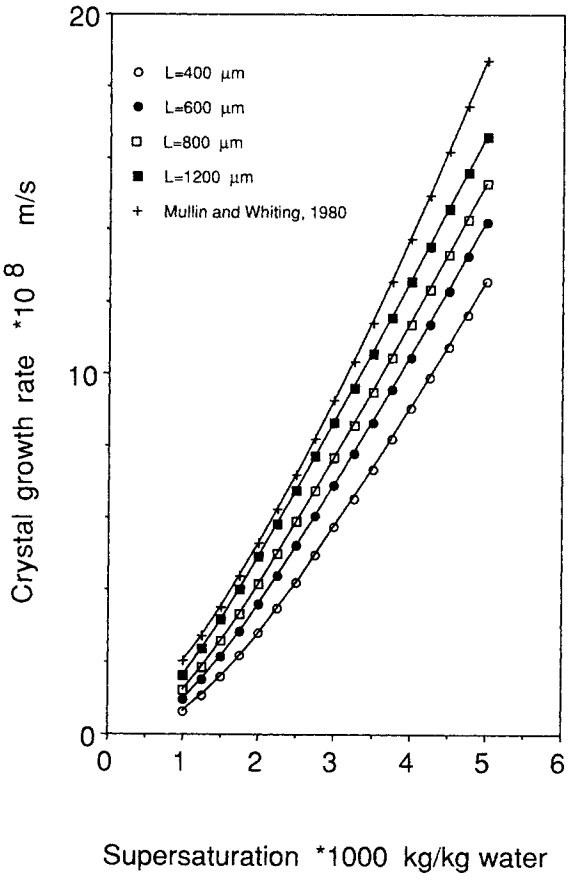


**Figure 9. Comparison of the crystal growth rate with previous published data, $E_v = 16.7$ kJ/mol.**

distinguish from each other. Size effects observed in this study are due significantly to using seed particles of different sizes. Therefore, we interpret the results as size dependency. Possible mechanisms of size-dependent surface integration rates are discussed by Garside et al. (1974) and by Garside et al. (1976). It has been suggested (recently adopted by Budz et al., 1984; Tai and Yu, 1989) that particle collisions, depending on the number of particles, energy and particle size, may influence the number of dislocations. However, this theory would not explain the size-dependent growth observed in fixed single-crystal experiments by Herndon and Kirwan, (1982). Garside et al. (1974) consider the hydrodynamics in their fluidized-bed experiments to be too mild to fit into this model. No clear influence of seed amount is observed in our results but the magma density is always low. We found the order of the surface integration rate with respect to crystal size to be approximately 1.6. This value is higher than those found by others for other substances; for instance, 0.7 (Garside et al., 1974) and 0.27 (Tavare and Chivate, 1979) for potassium sulfate, 0.38–0.53 for potash alum (Garside and Jancic, 1976; Garside et al., 1974), and 0.5 for nickel sulfate (Phillips and Epstein, 1974). If an overall power law relation is used (Eq. 23) the order of the size dependency in the present study becomes approximately 0.5.

Usually, crystal growth rates are correlated and described by simple overall power law equations. In using the two-step approach it has recently been suggested to arbitrarily define the order of the surface integration rate to 2. This would significantly simplify the parameter estimation. However, there is an obvious difference between correlation of experimental data covering a limited range and describing the actual process accurately enough to allow for extrapolations. All experiments of the present study, using the nonlinear optimization technique, may be well correlated by a simple overall power law expression:

$$G = 20.93\Delta c^{1.821} L^{0.4754} N^{0.3634} \exp(-18071/RT) \quad (23)$$

The sum of squared residuals is only somewhat higher ($F = 7.3 \times 10^{-6}$) than the value for Eq. 19. The number of parameters to fit is five in both cases. In Figure 10 we compare Eqs. 19 and 23 as a function of supersaturation. The stirring rate, the crystal size, and the temperature are extrapolated outside the experimental range. The shadowed area shows the range of estimated experimental uncertainty and the range of supersaturation covered in the experiments. Within the range of experiments and the range of experimental uncertainty, the power law equation is quite applicable. The diagram, however, reveals that, outside the experimental range but well within reasonable values for different parameters, significant differences occur between the power law expression and the two-step model. The power law expression may predict twice as high growth rates as the two-step model. If the growth rate order is fixed to $r = 2$ in Eq. 19, and the regression analysis is performed to extract the remaining four parameters using $E_v = 16.7$ kJ/mol, the goodness of fit decreases somewhat: $F = 7.4 \times 10^{-6}$.

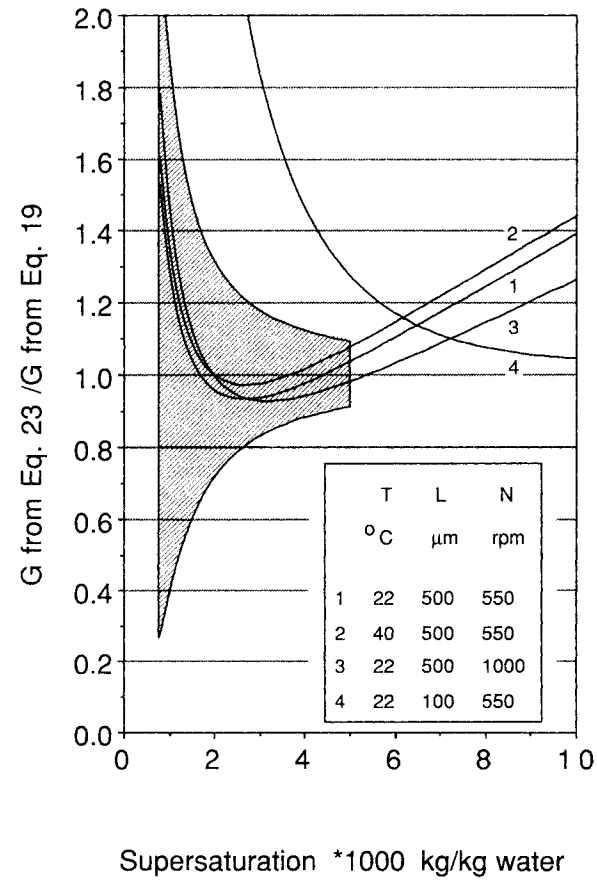


**Figure 10. Comparison of the two-step model with $E_v = 16.7$ kJ/mol and the power law equation.**

However, more important is the fact that the values of the four parameters change significantly: $k_{d0} = 4.0 \times 10^{-2}$ m/s, $k_{r0} = 3.48 \times 10^{+3}$, $b = 0.69$, and $E_r = 18$ kJ/mol, obviously reducing the physical meaning. In Figure 11 we compare the two-step equation applying $r = 2$ and Eq. 19 in which also $r$ is determined from the experimental results. As was the case for the power law expression, the agreement is good within the range of experimental data, but significant deviations occur when extrapolating outside the experimental range.

## Conclusions

Growth and dissolution rates of succinic acid crystals in an aqueous solution have been measured in a laboratory, stirred-tank crystallizer. The concentration change in isothermal, seeded experiments is recorded. An improved method of evaluating the crystal growth rate parameters is developed and used. A two-step growth rate function is fitted directly to the supersaturation measurements using a desupersaturation balance and nonlinear optimization procedures. Thus uncertainties introduced by the traditional correlation of the concentration vs. time curve are circumvented. The five-parameter optimization is shown to produce physically meaningful values. In the range studied, the growth rate is controlled by both volume diffusion and surface integration resistances. The order of the surface integration with respect to supersaturation is approximately 3, and the process is size-dependent. When extrapolating outside the range of experiments, the two-step equation is shown to predict growth rates that are significantly different from those predicted by a corresponding power law expression. The dissolution rate shows a nonlinear dependence on undersaturation. This effect may be explained by changes in crystal shape during dissolution. The initial dissolution rate constant of each experiment is in good agreement with the corresponding volume diffusion rate constant for crystal growth.

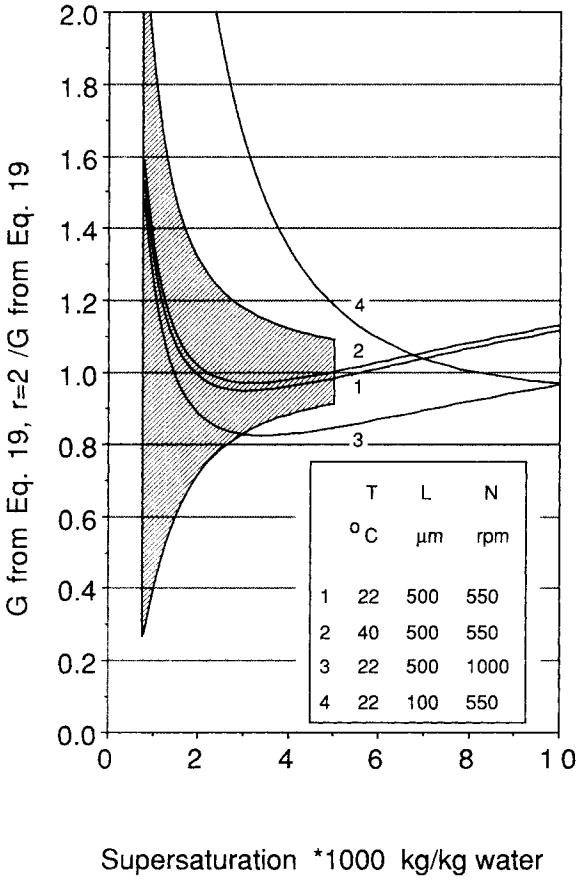


**Figure 11. Comparison of the two-step model and the model with $r = 2$, $E_r = 16.7$ kJ/mol.**


## Acknowledgment

The financial support of The Swedish Board for Technical Development (STU), The Swedish Council for Planning and Coordination of Research (FRN), and The Swedish Industrial Association for Crystallization Research and Development (IKF) are gratefully acknowledged.


## Notation

$c$ = concentration of the solution, kg/kg solvent
$c_i$ = interfacial concentration, kg/kg solvent
$c^*$ = solubility, kg/kg solvent
$\Delta c$ = concentration driving force, kg/kg solvent
= $c - c^*$ for growth, $c^* - c$ for dissolution
$\Delta c_0$ = initial concentration driving force, kg/kg solvent
$D$ = dissolution rate, m/s
$d$ = order for dissolution
$D_s$ = stirrer diameter, m
$D_t$ = tank diameter, m
$D_v$ = diffusivity, $m^2/s$
$E_r$ = activation energy of surface integration, J · $gmol^{-1}$
$E_v$ = activation energy of diffusion, J · $gmol^{-1}$
$F$ = sum of squares of residuals, $(kg/kg\ solvent)^2$
$G$ = linear crystal growth rate, m/s
$g$ = order for power law equation
$k_A$ = surface shape factor
$k_c$ = mass transfer coefficient, m/s
$k_D$ = mass transfer coefficient for dissolution, m/s (kg/kg solvent)
$k_D'$ = coefficient in Eq. 22
$k_d$ = mass transfer coefficient for crystal growth, m/s (kg/kg solvent)
$k_{d0}$ = mass transfer coefficient at 400 rpm, m/s (kg/kg solvent)
$k_g$ = coefficient for power law equation
$k_i$ = any kinetic parameter
$k_r$ = surface integration constant
$k_{r0}$ = surface integration constant, Eq. 19
$k_V$ = volume shape factor
$L$ = characteristic size of crystal, m
$L_0$ = size of seeds, m
$M$ = mass of solvent, kg
$m$ = number of the measured desupersaturation data in an experiment
$N$ = impeller rotation speed, rpm
$n$ = number of experiments used in the parameter estimation
$R$ = gas law constant, 8.314 J · $gmol^{-1}$ · $K^{-1}$
$r$ = order of surface integration
$T$ = temperature, K
$t$ = time, s
$W$ = mass of crystals, kg
$W_0$ = mass of seeds, kg

### *Greek letters*

$\rho$ = density of solution, $kg/m^3$
$\rho_c$ = density of crystal, $kg/m^3$
$\rho_w$ = density of water, $kg/m^3$
$\eta_r$ = surface integration effectiveness factor
$\nu$ = kinematic viscosity, $m^2/s$
$\epsilon$ = energy dissipation rate per unit mass, J/s kg

## Literature Cited


Bard, Y., *Nonlinear Parameter Estimation,* Academic Press (1974)
Bransom, S. H., and W. J. Dunning, "Kinetics of Crystallization, Part II," Discussions Faraday Society, No. 5, 96 (1949).

Budz, J., P. H. Karpinski, and Z. Naruc, "Influence of Hydrodynamics on Crystal Growth and Dissolution in a Fluidized Bed," *AIChE J,* **30**(5), 710 (1984).
———, "Effect of Temperature on Crystallization and Dissolution Processes in a Fluidized Bed," *AIChE J.*, **31**(2), 259 (1985).
Bujac, P. D. B., and J. W. Mullin, "A Rapid Method for the Measurement of Crystal Growth Rates in a Fluidized Bed Crystallizer," *Symp. Ind. Crystall.*, The Institution of Chemical Engineers, London, 121 (Apr., 1969).
Burton, W. K., N. Cabrera, and F. C. Frank, "The Growth of Crystals and the Equilibrium Structure of Their Surfaces," *Phil. Trans. Roy. Soc. London,* **243**(A), 299 (1951).
Chianese, A., A. Condo, and B. Mazzarotta, "The Growth and Dissolution of Sodium Perborate Crystals in a Fluidized Bed Crystallizer," *J. Crystal Growth,* **97,** 375 (1989).
Dahlquist, G., and Å. Björck, *Numerical Methods,* Prentice-Hall, Englewood Cliffs, NJ (1974).
Davey, R. J., J. W. Mullin, and M. J. L. Whiting, "Habit Modification of Succinic Acid Crystals Grown from Different Solvents," *J. Crystal Growth,* **58,** 304 (1982).
Draper, N. R., and H. Smith, *Applied Regression Analysis,* 2nd ed., Wiley (1981).
Garside, J., "The Concept of Effectiveness Factors in Crystal Growth," *Chem. Eng. Sci.*, **26,** 1425 (1971).
Garside, J., L. G. Gibilaro, and N. S. Tavare, "Evaluation of Crystal Growth Kinetics from a Desupersaturation Curve Using Initial Derivatives," *Chem. Eng. Sci.*, **37,** 1625 (1982).
Garside, J., and S. J. Jancic, "Growth and Dissolution of Potash Alum Crystals in the Subsieve Size Range," *AIChE J.*, **22**(5), 887 (1976).
Garside, J., R. Janssen-van Rosmalen, and P. Bennema, "Verification of Crystal Growth Rate Equations," *J. Crystal Growth,* **29,** 353 (1975).
Garside, J., and J. W. Mullin, "The Crystallization of Aluminum Potassium Sulphate: A Study in the Assessment of Crystallizer Design Data: III. Growth and dissolution rates," *Trans. IChemE,* **46,** T11 (1968).
Garside, J., J. W. Mullin, and S. N. Das, "Growth and Dissolution Kinetics of Potassium Sulphate Crystals in an Agitated Vessel," *Ind. Eng. Chem. Fund.*, **13**(4), 299 (1974).
Garside, J., V. R. Phillips, and M. B. Shah, "On Size-Dependent Crystal Growth," *Ind. Eng. Chem. Fund.*, **15**(3), 230 (1976).
Gilmer, G. H., and P. Bennema, "Computer Simulation of Crystal Surface Structure and Growth Kinetics," *J. Crystal Growth,* 13/14, 148 (1972).
Halfon, A., and S. Kaliaguine, "Alumina Trihydrate Crystallization, Part 1. Secondary Nucleation and Growth Rate Kinetics," *Can. J. Chem. Eng.*, **54,** 160 (1976).
Herndon, R. C., and D. J. Kirwan, "Size-Dependent Single Crystal Growth Kinetics," *AIChE Symp. Ser.*, **78**(215), 19 (1982).
Ishii, T., and S. Fujita, "Dissolution and Growth Rates of Crystal Particles in Stirred Tanks," *Kagaku Kogaku,* **29**(5), 316 (1965).
Jancic, S. J., and P. A. M. Grootscholten, *Industrial Crystallization,* Delft University Press (1984).
Jones, A. G., and J. W. Mullin, "Crystallization Kinetics of Potassium Sulphate in a Draft-tube Agitated Vessel," *Trans. Instn. Chem. Engrs.*, **51,** 302 (1973).
Karpinski, P., "Mass Crystallization in a Fluidized Bed," Inst. of Chem. Eng. and Heat Systems, No. 40, Monographs No. 22, Technical Univ. of Wroclaw, Wroclaw, Poland (1981).
Karpinski, P. H., "Importance of the Two-Step Crystal Growth Model," *Chem. Eng. Sci.*, **40**(4), 641 (1985).
Klug, D. L., and R. L. Pigford, "The Probability Distribution of Growth Rates of Anhydrous Sodium Sulfate Crystals," *Ind. Eng. Chem. Res.*, **28,** 1718 (1989).
Levins, D. M., and J. R. Glastonbury, "Particle-Liquid Hydrodynamics and Mass Transfer in a Stirred Vessel," *Trans. Instn. Chem. Engrs.*, **50,** 132 (1972).
Misra, C., and E. T. White, "Kinetics of Crystallization of Aluminum Trihydroxide from Seeded Caustic Aluminate Solutions," *Chem. Eng. Prog. Symp. Ser.*, **67**(110), 53 (1971).
Mullin, J. W., *Crystallization,* 2nd ed., Butterworths, London (1972).
Mullin, J. W., and C. Gaska, "The Growth and Dissolution of Potassium Sulphate Crystals in a Fluidized Bed Crystallizer," *Can. J. Chem. Eng.*, **47,** 483 (1969).
Mullin, J. W., and M. J. L. Whiting, "Succinic Acid Crystal Growth Rates in Aqueous Solution," *Ind. Eng. Chem. Fund.*, **19,** 117 (1980).
Oldshue, J. Y., *Fluid Mixing Technology,* McGraw-Hill, New York (1983).
Palwe, B. G., M. R. Chivate, and N. S. Tavare, "Growth Kinetics of Potassium Sulphate Crystals in a DTB Agitated Crystallizer," *Chem. Eng. Sci.*, **39,** 903 (1984).
Palwe, B. G., M. R. Chivate, and N. S. Tavare, "Growth Kinetics of Ammonium Nitrate Crystals in a Draft Tube Baffled Agitated Batch Crystallizer," *Ind. Eng. Chem. Process Des. Dev.*, **24,** 914 (1985).
Phillips, V. R., and N. Epstein, "Growth of Nickel Sulphate in a Laboratory-Scale Fluidized-Bed Crystallizer," *AIChE J.*, **20**(4), 678 (1974).
Scrutton, A., and P. A. M. Grootscholten, "A Study on the Dissolution and Growth of Sodium Chloride Crystals," *Trans. IChemE,* **59,** 238 (1981).
Seidell, A., *Solubilities of Inorganic and Metalorganic Compounds: I,* 4th ed., van Nostrand Co., Princeton (1958).
Stephen, H., and T. Stephen, *Solubilities of Inorganic and Organic Compounds: 1,* Part 1, Pergamon Press, Oxford (1963).
Tai, C. Y., and C. H. Lin, "Crystal Growth Kinetics of the Two-Step Model," *J. Crystal Growth,* **82,** 377 (1987).
Tai, C. Y., and K. H. Yu, "Growth Kinetics of Potassium Alum Crystal in a Well-Agitated Vessel," *J. Crystal Growth,* **96,** 849 (1989).
Tanimoto, A., K. Kobayashi, and S. Fujita, "Overall Crystallization Rate of Copper Sulfate Pentahydrate in an Agitated Vessel," *Int. Chem. Eng.*, **4**(1), 153 (1964).
Tavare, N. S., and M. R. Chivate, "Growth and Dissolution Kinetics of Potassium Sulphate Crystals in a Fluidized Bed Crystallizer," *Trans. IChemE,* **57,** 35 (1979).
Tavare, N. S., and J. Garside, "Simultaneous Estimation of Crystal Nucleation and Growth Kinetics from Batch Experiments," *Chem. Eng. Res. Des.*, **64,** 109 (1986).
Verigin, A. N., I. A. Shchuplyak, M. F. Mikhalev, and V. N. Kulikov, "Investigation of Crystallization Kinetics with Programmed Variation of the Solution Temperature," *Zhurnal Prikladnoi Khimii,* **52**(8), 1898 (1979).

*Manuscript received Sept. 5, 1989, and revision received Feb. 8, 1990.*